Optimising height-growth predicts trait responses to water availability and other environmental drivers

Isaac R. Towers[1,*] (ORCID ID:https://orcid.org/0000-0003-4570-3474),
Andrew O'Reilly-Nugent[1,**],
Manon E.B. Sabot[2,3],
Peter A. Vesk[4] (https://orcid.org/0000-0003-2008-7062),
Daniel S. Falster[1] (https://orcid.org/0000-0002-9814-092X)

February 1, 2024

[1] The School of Biological, Earth and Environmental Sciences, The University of New South Wales, NSW, 2052, Australia
[2] Max Planck Insitute for Biogeochemistry, 07745 Jena, Germany
[3] ARC Centre of Excellence for Climate Extremes and Climate Change Research Centre, The University of New South Wales, NSW, 2052, Australia
[4] School of Agriculture, Food and Ecosystem Sciences, The University of Melbourne, Parkville, VIC, 3010, Australia
[*] Corresponding author: isaac.towers1@unsw.edu.au
[**] Current address: Climate Friendly, Sydney, NSW, 2052, Australia
Keywords: leaf mass per area, huber value, wood density, sapwood-specific conductivity, eco-evolutionary optimality, stomata, hydraulics, trait change

Running title: Plant trait response to soil moisture

Word count: 8050

1 Supporting Information

1.1 Supporting Information Methods

1.1.1 Photosynthesis model

Net photosynthesis, P_{net}, was modelled using a standard coupled stomatal-photosythnesis model, which equates photosynthetic demand for CO_2, P_{net}, with the diffusive supply of CO_2:

$$P_{net}(C_\mathrm{i}) = g_c(\psi_\mathrm{leaf})\frac{(C_\mathrm{a} - C_\mathrm{i})}{P_\mathrm{atm}}, \tag{1}$$

In turn, P_{net} is modelled according to the Farquhar biochemical model (Farquhar *et al.* 1980) which includes a smoothed hyperbolic transition between two limiting rates of photosynthesis, being the Rubisco-limited rate (A_c) and the electron-transport limited rate (A_j):

$$P_{net} = \frac{A_c + A_j - \sqrt{(A_c + A_j)^2 - 4hA_cA_j}}{2h} - R_d, \tag{2}$$

where h is the curvature factor of the smoothing function and R_d is leaf-level respiration.

A_c is defined as:

$$A_c = \frac{V_{c,max}(C_i - \Gamma^*)}{C_i + K_m}, \tag{3}$$

and A_j is defined as:

$$A_j = \frac{J(C_i - \Gamma^*)}{4(C_i + 2\Gamma^*)}, \tag{4}$$

where $V_{c,max}$ is the maximum velocity of carboxylation, C_i is the intercellular partial pressure of CO_2 and Γ^* is the CO_2 compensation point.

K_m is the Michaelis-Menten constant for photosythnesis and is described as:

$$K_m = K_c\left(1 + \frac{O_a}{K_o}\right), \tag{5}$$

where K_c and K_o are the Michaelis-Menten constants for CO_2 and O_2, respectively and O_a is the atmospheric concentration of O_2 in terms of partial pressure.

J describes the joint dependency of A_j on irradiance, I and the maximum electron transport rate, J_{max}:

$$J = \frac{aI + J_{max} - \sqrt{(aI + J_{max})^2 - 4caIJ_{max}}}{2c}, \tag{6}$$

where a is the quantam yield of electron transport and c is the curvature of the relationship between J and I.

$V_{c,max}$, J_{max}, Γ^*, K_c and K_o have temperature-dependencies according to Arrhenius functions. However, because we do not consider the explicit effect of temperature in the present analysis, we assume that these parameters are fixed at their 25°C values (i.e. $V_{c,max} = V_{c,max,25}$) (Bernacchi *et al.* 2001).

1.1.2 Leaf respiration

In the FF16w physiological module, leaf respiration per unit mass leaf (r_l; $mol\ kg^{-1}\ s^{-1}$) is assumed to be the summed component of respiration associated with nitrogen allocated to photosynthetic capacity $r_{l,p}$ and nitrogen allocated to structural components of the leaf $r_{l,s}$:

$$r_l = r_{l,s} + r_{l,p}. \tag{7}$$

Dong *et al.* (2022) show that for woody, non-nitrogen fixers, N_{area} can be linearly predicted as a function of $V_{cmax,25}$ and ϕ:

$$N_{area} = \alpha + \beta_1\phi + \beta_2 V_{c,max}. \tag{8}$$

The β terms describes how N_{area} changes with unit increases in either ϕ of $V_{c,max}$ and α is the intercept value of this equation. Estimation of β_2 from a global dataset indicates that this term corresponds with the relative mass contribution of Rubisco and cytochrome

f to $V_{c,max}$ and J_{max} per unit mass increase in $V_{c,max}$, assuming as we do here, that $V_{c,max,25}$ and J_{max} occur in the leaf at a ratio of approximately 2:1 (Smith & Keenan 2020; Dong *et al.* 2022).

Assuming that α accounts for structural components of N_{area} not accounted for by ϕ, it can be argued that:

$$N_{mass,s} = (\alpha + \beta_1\phi)\phi^{-1}, \tag{9}$$

and that,

$$N_{mass,p} = (\beta_2 V_{c,max})\phi^{-1}. \tag{10}$$

Then, N_{mass} is multiplied by R, the rate of respiration per unit mass nitrogen to give:

$$r_{l,s} = R_{l,s}N_{mass,s}, \tag{11}$$

and,

$$r_{l,p} = R_{l,p}N_{mass,p}. \tag{12}$$

Importantly, $R_{l,s}$ and $R_{l,p}$ can be different values, reflecting possible differentiation in the repspiration rate of a given mass of structural versus photosynthetic nitrogen.

1.2 Supporting Information Tables

Table S1: **Variable descriptions, tested parameter values and units in the Supplementary Information Methods**.

Symbol	Description	Tested values	Units
Parameter			
$K_{c,25}$	Michaelis-Menten constant (carboxylation)	404.9	μmol mol^{-1}
$K_{o,25}$	Michaelis-Menten constant (oxygenation)	278.4	mmol mol^{-1}
Γ^*_{25}	CO_2 compensation point	42.75	μmol mol^{-1}
h	Curvature factor	0.99	unitless
$N_{mass,s}$	Structural nitrogen mass per leaf mass	Derived from ϕ	kg N kg^{-1}
$N_{mass,p}$	Photosynthetic nitrogen mass per leaf mass	Derived from ϕ, $V_{c,max}$	kg N kg^{-1}
$R_{l,p}$	Respiration per unit mass photosynthetic nitrogen	40000	mol yr^{-1} kg N^{-1}
$R_{l,s}$	Respiration per unit mass structural nitrogen	21000	mol yr^{-1} kg N^{-1}
$r_{l,p}$	Respiration per unit mass leaf associated with photosynthetic nitrogen	Derived from $N_{mass,p}$, $R_{l,p}$	mol yr^{-1} kg^{-1}
$r_{l,s}$	Respiration per unit mass leaf associated with structural nitrogen	Derived from $N_{mass,s}$, $R_{l,p}$	mol yr^{-1} kg^{-1}
α	Intercept of N_{area} empirical relationship	0.535[a]	unitless
β_1	Linear coefficient for ϕ in N_{area} empirical relationship	0.009[a]	unitless
β_2	Linear coefficient for $V_{c,max}$ in N_{area} empirical relationship	0.006[a]	unitless

[a] Dong *et al.* (2022)

1.3 Supporting Information Figures

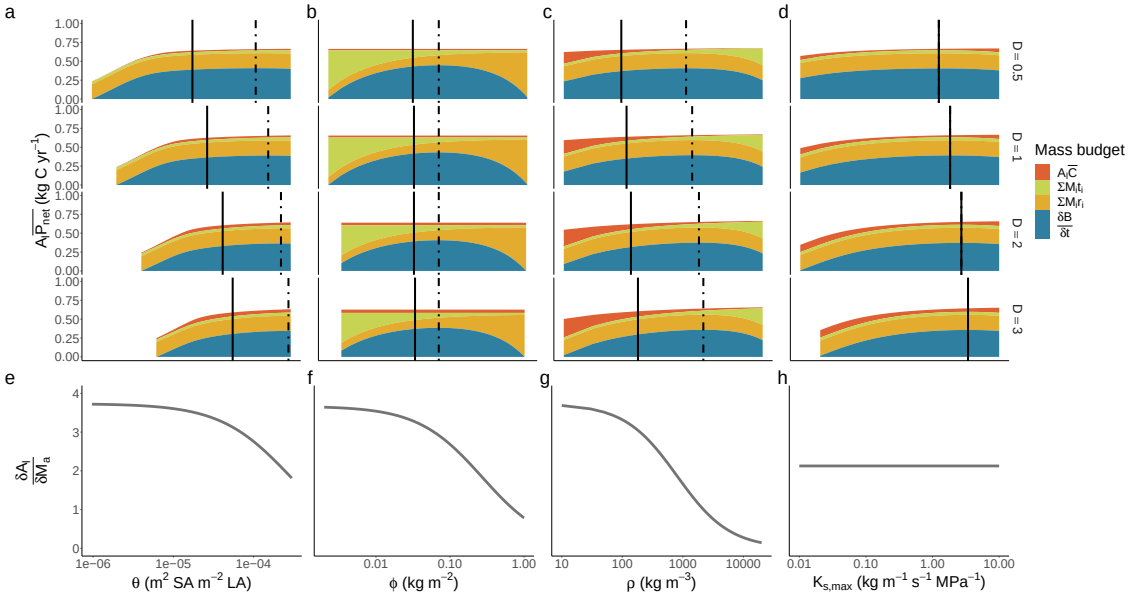

Figure S1: **Decomposition of the components determining trait optima across a vapour pressure deficit (D) gradient**. The top row of panels shows how net biomass production, $\frac{\mathrm{d}B}{\mathrm{d}t}$ emerges for each trait across an increasing vapour pressure deficit gradient (i.e. from the top to the bottom of panels **a-d**) as the residual of total assimilation, $(A_l\bar{P_{net}})$, after accounting for hydraulic costs, $A_l\bar{C}$, turnover $\sum M_i t_i$ and respiration $\sum M_i r_i$ of each plant tissue, i. The trait value maximising $\frac{\mathrm{d}B}{\mathrm{d}t}$ is indicated by the dashed vertical bar. The solid vertical line indicates the trait value maximising the height-growth rate, $\frac{dH}{dt}$. The $\frac{dH}{dt}$ optima emerges through multiplication of $\frac{dB}{dt}$ with the rate of leaf area deployment per unit of live mass growth $\frac{\mathrm{d}A_l}{\mathrm{d}M_a}$, shown in the second column. For most traits, this causes the $\frac{dH}{dt}$ optima to be lower than the $\frac{dB}{dt}$ optima, owing to the greater value of $\frac{\mathrm{d}A_l}{\mathrm{d}M_a}$ at low trait values in panels **e-g** but also explains why the optima are equivalent for $K_{s,max}$.

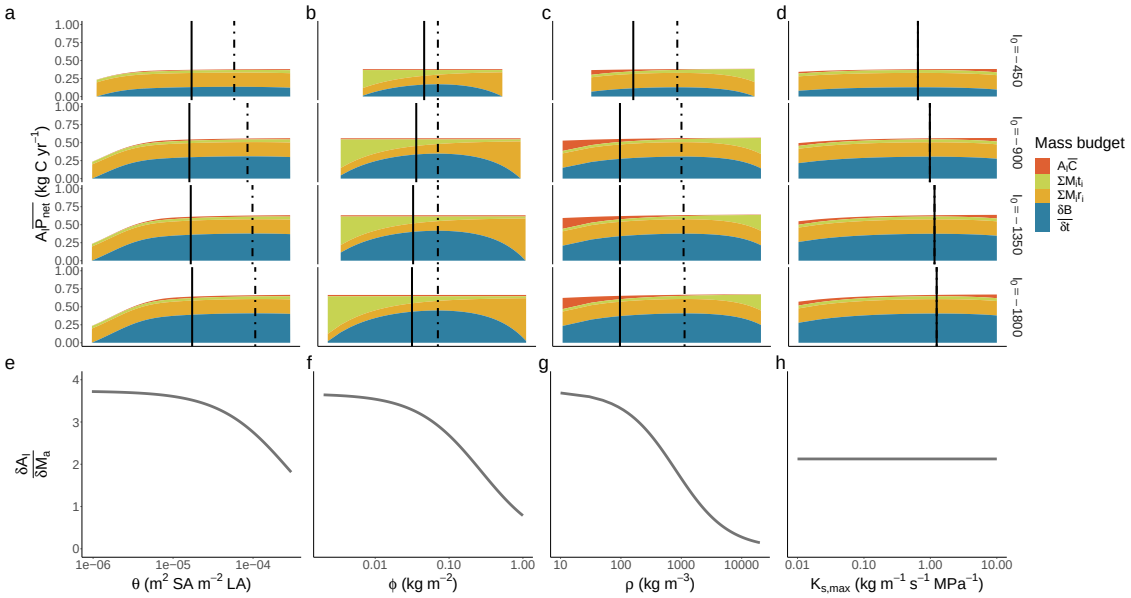

Figure S2: **Decomposition of the components determining trait optima across a above-canopy photon plux density (I_0) gradient**. The top row of panels shows how net biomass production, $\frac{\mathrm{d}B}{\mathrm{d}t}$ emerges for each trait across a increasing light availability gradient (i.e. from the top to the bottom of panels **a-d**) as the residual of total assimilation, ($A_l\bar{P_{net}}$), after accounting for hydraulic costs, $A_l\bar{C}$, turnover $\sum M_i t_i$ and respiration $\sum M_i r_i$ of each plant tissue, i. The trait value maximising $\frac{\mathrm{d}B}{\mathrm{d}t}$ is indicated by the dashed vertical bar. The solid vertical line indicates the trait value maximising the height-growth rate, $\frac{dH}{dt}$. The $\frac{dH}{dt}$ optima emerges through multiplication of $\frac{dB}{dt}$ with the rate of leaf area deployment per unit of live mass growth $\frac{\mathrm{d}A_l}{\mathrm{d}M_a}$, shown in the second column. For most traits, this causes the $\frac{dH}{dt}$ optima to be lower than the $\frac{dB}{dt}$ optima, owing to the greater value of $\frac{\mathrm{d}A_l}{\mathrm{d}M_a}$ at low trait values in panels **e-g** but also explains why the optima are equivalent for $K_{s,max}$.

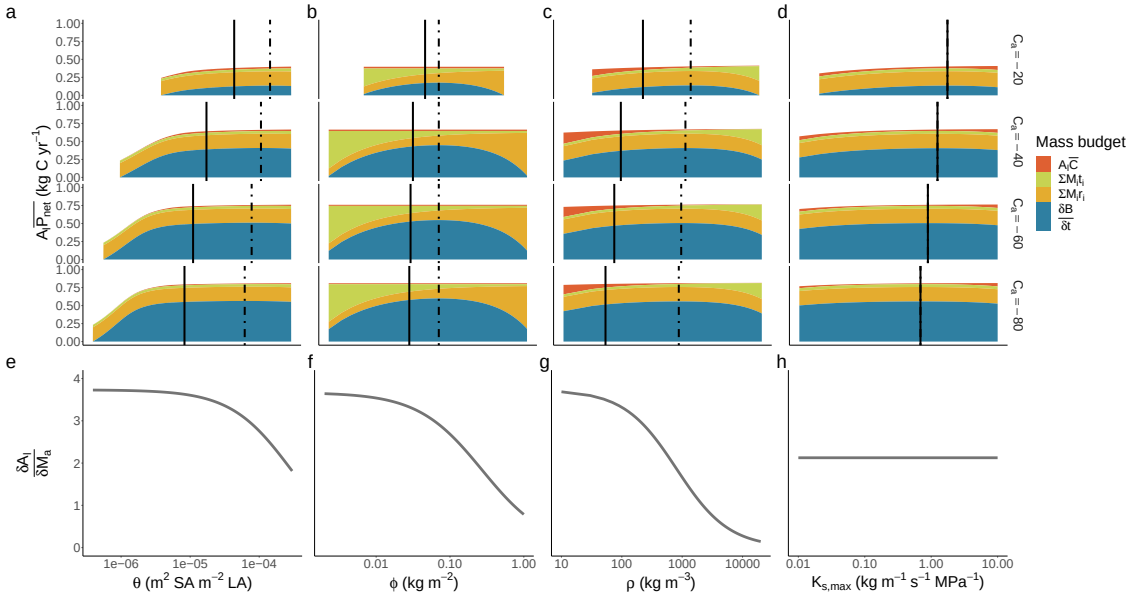

Figure S3: **Decomposition of the components determining trait optima across a atmospheric CO_2 gradient** (C_a). The top row of panels shows how net biomass production, $\frac{dB}{dt}$ emerges for each trait across an increasing atmospheric concentration of CO_2 (i.e. from the top to the bottom of panels **a-d**) as the residual of total assimilation, ($A_l\bar{P_{net}}$), after accounting for hydraulic costs, $A_l\bar{C}$, turnover $\sum M_i t_i$ and respiration $\sum M_i r_i$ of each plant tissue, i. The trait value maximising $\frac{dB}{dt}$ is indicated by the dashed vertical bar. The solid vertical line indicates the trait value maximising the height-growth rate, $\frac{dH}{dt}$. The $\frac{dH}{dt}$ optima emerges through multiplication of $\frac{dB}{dt}$ with the rate of leaf area deployment per unit of live mass growth $\frac{dA_l}{dM_a}$, shown in the second column. For most traits, this causes the $\frac{dH}{dt}$ optima to be lower than the $\frac{dB}{dt}$ optima, owing to the greater value of $\frac{dA_l}{dM_a}$ at low trait values in panels **e-g** but also explains why the optima are equivalent for $K_{s,max}$.

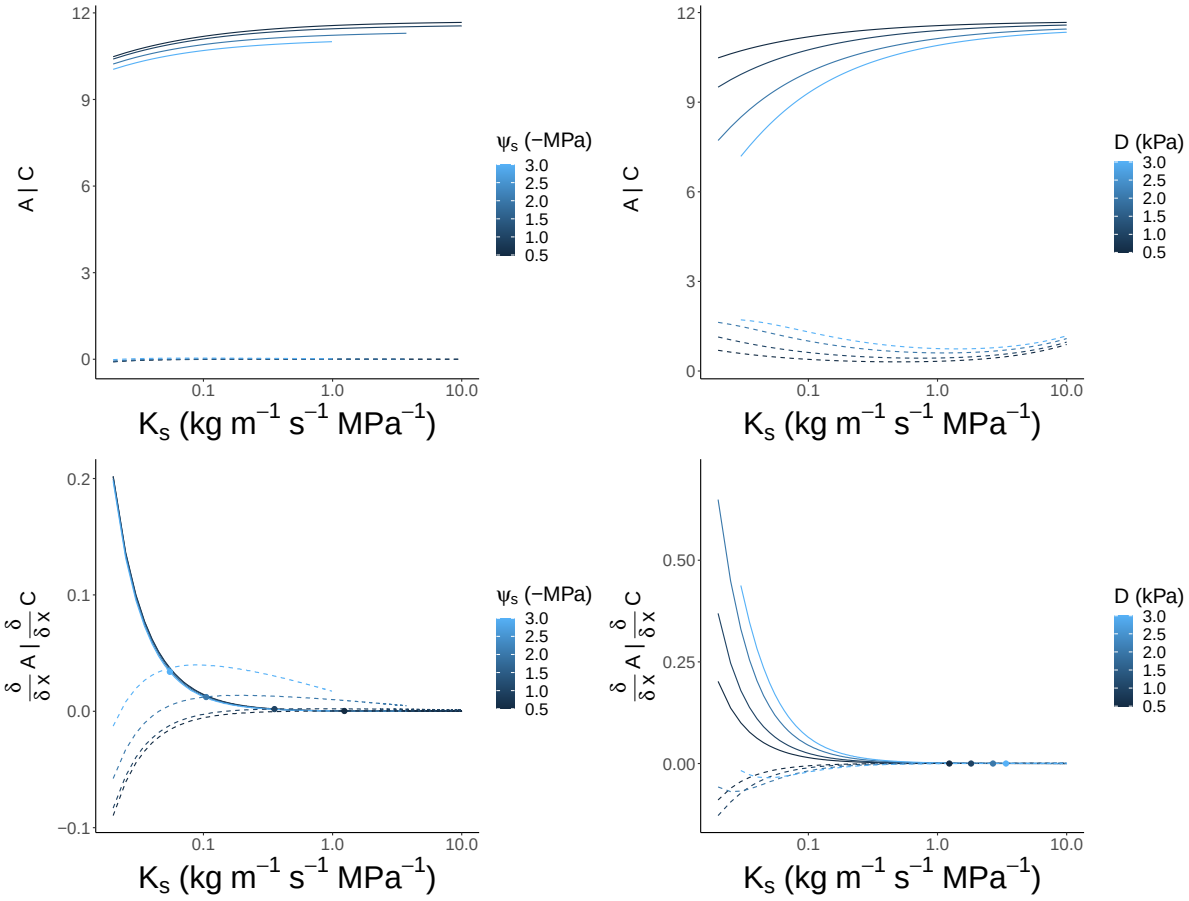

Figure S4: Graphical explanation for the response of $K_{s,max}$ to soil water availability (ψ_{soil} and atmospheric vapour pressure deficit (D). In the top row of plots, the optimal photosynthetic assimilation (A; solid lines) and hydraulic costs (C; dotted lines) from the stomatal model for a given set of traits (x) are plotted with respect to variation in $K_{s,max}$. Colour shading indicates the environmental conditions that the stomatal model was optimised under. In the bottom row of plots, the same curves derived with respect to variation in $K_{s,max}$ are illustrated. The optimum $K_{s,max}$ under each environment is indicated by the coloured points and occurs where $\frac{\delta}{\delta x}A = \frac{\delta}{\delta x}C$ The left column of plots illustrates how $K_{s,max}$ increases as soils dry owing to an increase in the elevation of $\frac{\delta}{\delta x}C$. The right column of plots illustrates how $K_{s,max}$ increases with D owing primarily to an increase in the elevation of $\frac{\delta}{\delta x}A$, which occurs because A increases more rapidly with $K_{s,max}$ in drier atmospheres.

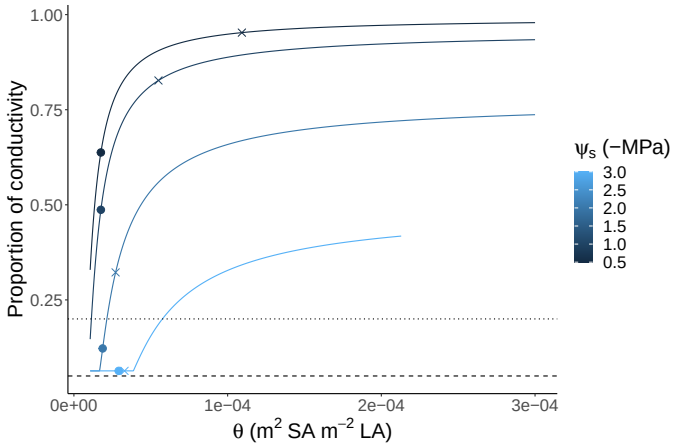

Figure S5: The proportion of conductivity in the xylem increases with the sapwood to leaf area ratio (θ) because ψ_{leaf} is less negative when the water transport rate is higher. As ψ_{soil} becomes more negative, the biomass production (crosses) and height-growth rate (circles) optimising values of θ decline, because the costs associated with greater sapwood are greater than the cost of losing hydraulic conductivity, except in very dry soils (lightest blue). The horizontal lines indicate losses of conductivity associated with a high risk of drought-based mortality (80%; Hammond *et al.* 2019) and catastrophic xylem failure (95%).

References

Bernacchi, C.J., Singsaas, E.L., Pimentel, C., Portis Jr, A.R. & Long, S.P. (2001) Improved temperature response functions for models of Rubisco-limited photosynthesis. *Plant, Cell & Environment* **24**, 253–259, _eprint: https://onlinelibrary.wiley.com/doi/pdf/10.1111/j.1365-3040.2001.00668.x.

Dong, N., Prentice, I.C., Wright, I.J., Wang, H., Atkin, O.K., Bloomfield, K.J., Domingues, T.F., Gleason, S.M., Maire, V., Onoda, Y., Poorter, H. & Smith, N.G. (2022) Leaf nitrogen from the perspective of optimal plant function. *Journal of Ecology* **110**, 2585–2602.

Farquhar, G.D., von Caemmerer, S. & Berry, J.A. (1980) A biochemical model of photosynthetic CO2 assimilation in leaves of C 3 species. *Planta* **149**, 78–90.

Hammond, W.M., Yu, K., Wilson, L.A., Will, R.E., Anderegg, W.R.L. & Adams, H.D. (2019) Dead or dying? Quantifying the point of no return from hydraulic failure in drought-induced tree mortality. *New Phytologist* **223**, 1834–1843, _eprint: https://onlinelibrary.wiley.com/doi/pdf/10.1111/nph.15922.

Smith, N.G. & Keenan, T.F. (2020) Mechanisms underlying leaf photosynthetic acclimation to warming and elevated CO2 as inferred from least-cost optimality theory. *Global Change Biology* **26**, 5202–5216, _eprint: https://onlinelibrary.wiley.com/doi/pdf/10.1111/gcb.15212.